



Localization and characterization of the metallic band gaps in a ternary metallo-dielectric photonic crystal

Adalberto Alejo-Molina*, David L. Romero-Antequera, José J. Sánchez-Mondragón

Instituto Nacional de Astrofísica, Óptica y Electrónica, Calle Luis Enrique Erro No. 1, Tonantzintla, Puebla, C.P. 72000, México

ARTICLE INFO

Article history:

Received 15 July 2013

Received in revised form

3 September 2013

Accepted 9 September 2013

Available online 23 September 2013

Keywords:

Photonic crystal

Metal

Band gap width

ABSTRACT

In this work, we demonstrate the existence of structural metallic band gaps in a ternary material, dielectric–dielectric–metal, and we show analytical equations for their computation. We show the existence of metallic band gaps not only in the lowest band but also for high frequencies. These gaps are structural ones but different and additional to the dielectric ones in the dielectric photonic crystal substrate. Therefore, as the desired properties of both, the dielectric and metallic photonic crystals, are present the applications for this particular structure are straightforward.

© 2013 Elsevier B.V. All rights reserved.

1. Introduction

Dielectric photonic crystals (DPC) have been widely studied experimentally [1] since Second World War under the concept of thin-films. Thin-films are very important because their direct application in optical filters, antireflection films and coatings, but all their development, was development were in some sense empiric knowledge of the materials and their combinations despite these kind of stratified media were first theoretical studied by Lord Rayleigh in 1887 [2].

Often, a stack formed of a dielectric material and a metallic layer is called metallic photonic crystal (MPC) [3–8]. In most of the related works, metallic layers are thin (less than the skin depth) and the dielectric material is air ($n_a = 1$). One of the first works in MPC was due to Kuzmiak and Maradudin [3]. They presented two methods to deal with the metallic components in the case of 1D-DPC, the transfer matrix method (TMM) model and the perturbative plane-wave method (PWM). These authors calculated band structure for thin metallic layers in a regime where band diagrams are still valid. In contrast, Yablonovitch and co-workers explored the opposite regimen of thick metallic layers where the inclusion of metal cannot be considered a perturbation and band structures are no longer valid.

The study of stacks could appear to be an old problem. However, new effects and interesting phenomena [9] could be studied and modeled in this “well-known” structure. For example, combinations of positive and negative indices [10,11], or linear with nonlinear and nonlinear–nonlinear stacks [12,13]. Also, new geometries, as for example Bragg fibers [14] or Bragg onion [15–17] can be explored beginning from the basic 1D-DPC. Only recently ternary systems in

PCs have started to be studied in their different combinations. Stacks formed by three dielectrics were also anticipated by Yeh [18] and now engineering of the gaps [19–23] is a topic of interest due to our actual technology and control of materials. Also, more complicated periodic structures have been investigated before, as for example, layered media with a sinusoidal index profile or exponential index profile. These special stacks can be thought as a medium made of many layers with different indices of refraction and they are called graded-index multilayer stack [24]. Moreover, quasiperiodic structures in one dimension were already explored, the more usuals are the Fibonacci quasicrystals [25–27]. These aperiodic structures are mentioned in this work because, interestingly, they presented some similarities with the transmittance of the structure proposed by us, as we will see later.

Therefore, in this work, we will discuss some features of the metallic photonic crystal described above and we will point out which of these features coexist in the structure that we are proposing, one dimensional metallo-dielectric photonic crystal (1D-MDPC) and we will show that there is a particular dominion where band structure and transmittance are complemented. The paper is organized as follows: in Section 2, a short review of the formalism for 1-D metallic and dielectric PCs is presented; Section 3 computes the relation dispersion for a 1D-MDPC; and Section 4 presents the analytical calculation of the gap location and gap width. Finally, some conclusions are drawn in Section 5.

2. A quick review of metallic and dielectric 1-D photonic crystals

As it is well-known, metals are highly dispersive and reflective in a wide range of frequencies, from microwave to far-infrared.

* Corresponding author. Tel.: +52 222 2663100; fax: +52 222 2472580.
E-mail address: adalberto_am@hotmail.com (A. Alejo-Molina).

Therefore, the penetration of electromagnetic waves into metals is negligible. But at higher frequencies towards the near-infrared and visible part of the spectrum, field penetration increases significantly and then dissipates too. In the range of ultraviolet frequencies, metals behave as dielectrics and allow the propagation of electromagnetic radiation. However there is still some degree of attenuation, depending on the metal itself. In the case of noble metals, as gold or silver, there is strong absorption in this regime mainly due to transitions between electronic bands.

The dispersive properties can be described via a complex dielectric function $\epsilon_m(\omega) = \epsilon_R(\omega) + i\epsilon_I(\omega)$. Thus, the index of the metal is given by $n_m = \epsilon_m(\omega)^{1/2}$, and can be modeled through

$$\epsilon_m(\omega) = 1 - \frac{\omega_p^2}{\omega(\omega + i\gamma)}, \quad (1)$$

which is the Drude model [3,4] with the following parameters: $\omega_p = 1.6 \times 10^{16}$ rad/s ($\lambda_p = 1180$ nm, medium-infrared) is the plasma frequency and $\gamma = 0.001\omega_p$ is the damping coefficient and it is related directly with absorption. These are typical values for metals such as copper, gold, silver and aluminum. The model is in good agreement with alkali metals up to the ultraviolet and provides an acceptable description of the dielectric constant (index of refraction plus absorption) for noble metals, in a range of frequencies that includes low-frequency, radio waves and high-frequency, near-ultraviolet light.

Using the transfer matrix method (TMM) [24], the dispersion relation for the dielectric PC is given by

$$f(k_1, k_2) = \cos(\kappa L) = \cos(k_1 a) \cos(k_2 b) - \frac{k_1^2 + k_2^2}{2k_1 k_2} \sin(k_1 a) \sin(k_2 b), \quad (2)$$

where κ is the Bloch wave number, the wave numbers k_i are defined in the usual way $k_i = (\omega/c)n_i$ ($i = 1, 2$). For a metallic binary stack the dispersion relation is the same as that in Eq. (2) but with the appropriate changes. For DPCs, where all the components are non-absorbent dielectric materials, the Bloch wave number is a pure real number in the frequency range of transmission bands in the first Brillouin zone. However, in the band gaps the Bloch wave number is complex, with the real part in the limit of the Brillouin zone and the imaginary part varying as a function of the frequency. In the boundaries of the Brillouin zone, $\text{Re}\{\kappa\} = \pi/L$, therefore

$$\kappa L = \pi \pm i x, \quad (3)$$

which means that the real part of the cosine function in the left part of Eq. (2) is close to 1 and the imaginary part x (absorption) will change in the band gap region, but in the boundaries will be zero. Also, there is a particular frequency ω_B (the Bragg frequency, in our numerical calculations was chosen as a telecommunication frequency, with the associated wavelength $\lambda_B = 1550$ nm) that satisfies

$$k_1 a = k_2 b = \frac{\pi}{2}, \quad (4)$$

which is located in the center of the band gap for a quarter-wave stack. Using conditions (3) and (4) in the dispersion relation (2), yields

$$x = \text{arc cosh} \left(\frac{k_1^2 + k_2^2}{2k_1 k_2} \right). \quad (5)$$

Using the identity $\text{arccos} \xi = \ln(\xi + \sqrt{\xi^2 - 1})$ ($\xi \geq 1$) and the expansion

$$\ln \xi = \ln \left(\frac{1+g}{1-g} \right) \approx 2g + \dots, \quad (6)$$

where $g = (\zeta - 1)/(\zeta + 1)$, we finally arrive to the usual form found in the literature

$$x = \text{arc cosh} \left(\frac{k_1^2 + k_2^2}{2k_1 k_2} \right) = \left| \ln \left(\frac{k_1}{k_2} \right) \right| \approx 2 \frac{|k_1 - k_2|}{k_1 + k_2}. \quad (7)$$

This equation gives the maximum value of the absorption in the center of the band gap. For the computation of the approximate width of the band gap, a small shift in the central frequency ω_B of the band gap is considered, thus

$$k_1 a = k_2 b = \frac{\pi}{2} + \epsilon, \quad (8)$$

additionally, the band gap is in the border of the Brillouin zone and consequently it should satisfy condition (3); therefore, the dispersion relation takes the form

$$\cos(\pi + ix) = \sin^2 \epsilon - \frac{k_1^2 + k_2^2}{2k_1 k_2} \cos^2 \epsilon. \quad (9)$$

Simplifying the trigonometric functions

$$\epsilon = \pm \arcsin \left(\frac{|k_1 - k_2|}{k_1 + k_2} \right) \approx \pm \frac{|k_1 - k_2|}{k_1 + k_2}. \quad (10)$$

Thus, the total band gap width, is given by

$$\Delta\omega_{Dgap} \approx \frac{2}{\pi} (2\epsilon) \omega_B = \frac{4|k_1 - k_2|}{\pi k_1 + k_2} \omega_B. \quad (11)$$

The previous procedure was discussed before by Yeh [24]. In the MPC case there is a complex wave number for the metal with real (imaginary) part $k_{2R}(k_{2I})$. In such a case, the real part of the Bloch wave number, κ_R , is associated with the index of refraction as well as the imaginary part κ_I is directly related to the absorption coefficient α .

Thus Eq. (2), for this MPC, was solved by previous authors [3–8] numerically to determine a complex band structure, which, in addition the dispersion relation curves $\omega = \omega(k)$, also yields the absorption coefficient α of the corresponding mode. From these previous works [3–8] it is known that there are two types of band gaps for this particular combination of dielectric and metal. The band gap at the bottom is mainly due to the absorption of the metal. There is a threshold frequency before which for low frequencies, almost all is absorbed. The other band gaps are structural band gaps, associated to the periodicity of the stack.

In summary, in the dielectric band gaps light is strongly reflected and in this way blocked at the end of the crystal, whereas in the metallic band gaps two different regimes are present: before the plasma frequency the light is strongly absorbed and after the plasma frequency there is still absorption but also the same effect which is present in pure dielectric crystals appears, generating in this way the metallic structural band gaps beyond the plasma frequency. Therefore, the inclusion of metal could be a disadvantage due to the absorption but at the same time this absorption could be an advantage if the device is designed as a filter for example.

On the other hand, some experimental research have been done for this specific MPC (air and metal). Scalora and co-workers [5] have shown that the structure remains transparent even if the total amount of metal is increased to hundreds of skin depths in net thickness. That is, the concept of skin depth loses its meaning in the case of a periodic structure where the presence of spatial discontinuities of the index of refraction alters the physical properties of the structure as a whole. Also, the coefficients of transmission and reflection could be engineered and the absorption is partially suppressed in the structure due to a coherent effect [28].

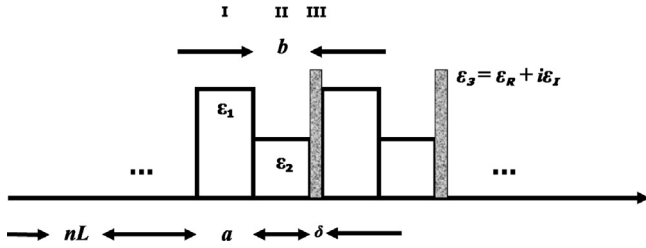


Fig. 1. Schematic representation of the MDPC stack. The DPC substrate is a quarter-wave stack of two different dielectrics with indices $n_1 = 3.58$ (Si) and $n_2 = 1.46$ (SiO₂).

3. One dimensional metallo-dielectric photonic crystal

The structure, that we proposed and investigated, is a 1D-MDPC formed of two dielectrics and metallic inserts. This is a ternary stack dielectric–dielectric–metal, *i.e.*, a DPC is used as a substrate and the metallic layers inserted do not modify the periodicity but the length of period. This also can be thought as the superposition of two different photonic crystals, one metallic and one dielectric, interestingly this idea was presented 2 years ago for 2D-DPC and the mean results of this research are: the resulting 2D-DPC could have a large complete band gap and the crystal is an aperiodic structure [29]. In constrast, as mentioned before, for 1D the stack is still a periodic structure. The stack is shown in Fig. 1 and the index of refraction has the profile

$$n(x) = \begin{cases} n_1, & nL \leq x < nL + a \\ n_2, & nL + a \leq x < nL + a + b \\ n_3, & nL + a + b \leq x < (n+1)L \end{cases}, \quad (12)$$

as well as it satisfies the periodicity relation

$$n(x) = n(x + L). \quad (13)$$

A feasible way to fabricate a device, with an equivalent behavior to the stack, is based on silicon on insulator (SOI) technology. An SOI wafer is formed by a thin silicon layer (Si) which is grown on top of a silicon dioxide layer (SiO₂). Using e-beam lithography we can develop a PMMA resist mask, to engrave the Si waveguide and the lateral grating in the Si layer at the same time. After the etching we perform a gold evaporation or sputtering with the sample inclined at a specific angle, which allow us to cover with gold only one side of the inner walls of the Si layer. After the gold is deposited, lift-off can be used to remove the remaining PMMA resist and hence gold was deposited on top of the PMMA resist. Finally, the whole structure can be covered with SiO₂ or a polymer with similar refractive index (see Fig. 2). A similar process can be used on InP based materials as demonstrated in Ref. [30].

The methodology followed to derive the dispersion relation and the transmittance of the system is the TMM, and it is discussed by us in another paper [28]. Among the interesting results summarized in that paper, we found that periodic metal array changes the concept of skin depth and partially suppresses the absorption as the field propagates within the material. This phenomena has its origin in a coherent feedback due to the periodicity of the structure and for the same reason to the discontinuities of the refraction index. Also, changes in the thickness of the metal, generate a full metallic stop gap which is thin at the beginning and gradually becomes thick. Furthermore, there is a shift in the central point of the stop gap and a broadening. The shift in the central point of the stop gap can be explained as a fundamental detuning, introduced in the resonance frequency due to the absorption or damping coefficient γ in Eq. (1). The broadening has its ground in the fact that the index of refraction of the metal is negative in a determinate range of frequencies and in this

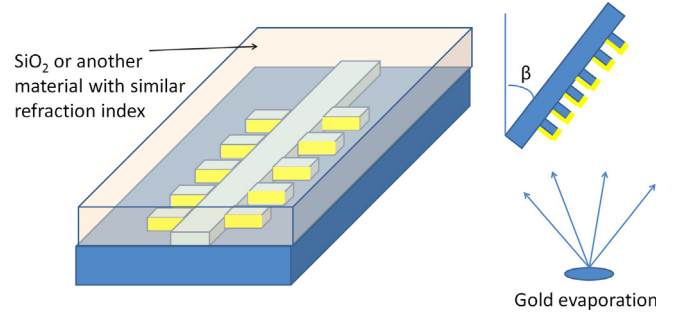


Fig. 2. One proposal for the experimental realization of the device. At the left the final waveguide and at the right the deposition of the metallic layer.

way, in average, the difference between the dielectric indices is larger. Then, as it is well-known, the larger the difference between the dielectric constants the bigger the stop gap and vice versa.

On the other hand, some of our early results were 1 year later corroborated by Wu et al. [22] in a very detailed study, and they show how the band gap width is modified by the presence of a metallic layer between two dielectric layers. They also studied the change in the band gap in function of the change in the plasma frequency and found the presence of omnidirectional band gaps for oblique incidence, all this in terms of the reflectance. Again, we agree with these authors in a conference paper presented in the same year [31] but we discuss our result in terms of band structure instead of reflectance. In contrast with their work, the structure that we proposed is a quarter-wave stack which has the bigger band gap possible for 1D photonic crystal for two fixed dielectrics [2]. Also, the band gap is centered exactly at the Bragg frequency of design. We are working in infrared and they are working in the visible range. Another big and very important difference is that we are using the same optical path length (which immediately means different thicknesses for two materials with a high contrast in their refraction index) and not the same physical thickness for the dielectric layers (which immediately means different optical path lengths for two materials with a high contrast in their refraction index). The ratio in the optical path length rules the periodicity of the transmittance even for the Fibonacci structures [25–27]. Therefore, our structure has higher symmetry for wave propagation, allowing us to describe it analytically, as follows.

The dispersion relation for the crystal described by Eq. (13) is given by

$$\cos[(\kappa_R + i\kappa_I)L] = \left[\cos(k_1 a) \cos(k_2 b) - \frac{1}{2} \frac{k_1^2 + k_2^2}{k_1 k_2} \sin(k_1 a) \sin(k_2 b) \right] \cos(k_3 \delta) - \frac{1}{2k_3} \left[\frac{k_1^2 + k_3^2}{k_1} \sin(k_1 a) \cos(k_2 b) + \frac{k_2^2 + k_3^2}{k_2} \cos(k_1 a) \sin(k_2 b) \right] \sin(k_3 \delta), \quad (14)$$

where the wave number is defined in the usual way

$$k_i = \frac{\omega}{c} n_i \quad (i = 1, 2, 3). \quad (15)$$

Considering $k_3 = k_{3R} + ik_{3I}$ given that n_3 follows the Drude model, the dispersion relation, Eq. (15), can be expressed as two non-redundant transcendental and coupled equations

$$p = \cos(\kappa_R L) \cosh(\kappa_I L) = f(k_1, k_2) \cos(k_{3R} \delta) \cosh(k_{3I} \delta) - \frac{1}{2|k_3|^2} \alpha [k_{3R} \sin(k_{3R} \delta) \cosh(k_{3I} \delta) + k_{3I} \cos(k_{3R} \delta) \sinh(k_{3I} \delta)] - \frac{1}{2k_1 k_2} \beta [k_{3R} \sin(k_{3R} \delta) \cosh(k_{3I} \delta) - k_{3I} \cos(k_{3R} \delta) \sinh(k_{3I} \delta)], \quad (16)$$

for the real part, and

$$\begin{aligned} q = & \sin(\kappa_R L) \sinh(\kappa_I L) = f(k_1, k_2) \sin(k_{3R} \delta) \sinh(k_{3I} \delta) \\ & + \frac{1}{2|k_3|^2} \alpha [k_{3R} \cos(k_{3R} \delta) \sinh(k_{3I} \delta) - k_{3I} \sin(k_{3R} \delta) \cosh(k_{3I} \delta)] \\ & + \frac{1}{2k_1 k_2} \beta [k_{3R} \cos(k_{3R} \delta) \sinh(k_{3I} \delta) + k_{3I} \sin(k_{3R} \delta) \cosh(k_{3I} \delta)], \end{aligned} \quad (17)$$

for the imaginary part. The function $f(k_1, k_2)$ is the original dispersion relation of the DPC substrate, Eq. (2), and α and β are given by the following expressions:

$$\alpha = k_1 \sin(k_1 a) \cos(k_2 b) + k_2 \cos(k_1 a) \sin(k_2 b), \quad (18)$$

$$\beta = k_2 \sin(k_1 a) \cos(k_2 b) + k_1 \cos(k_1 a) \sin(k_2 b). \quad (19)$$

It is possible to solve Eqs. (16) and (17) numerically. However, in our experience, it is not straightforward to provide an efficient solution in terms of computing time and solutions not always converge. Instead, we are going to propose an analytical solution which, to our knowledge, has not been provided before. The dispersion relation can be expressed as follows:

$$\cos[(\kappa_R + i\kappa_I)L] = p + iq, \quad (20)$$

where p and $q \in \mathbb{R}$. The inverse cosine function can be written as

$$\arccos w = \frac{\pi}{2} - \xi + \frac{i}{2} \ln \eta \quad (21)$$

where ξ is the magnitude of the complex number w , and η is the phase. It follows:

$$\kappa_R = \frac{1}{L} \left(\frac{\pi}{2} - \xi \right) = \frac{\pi}{2L} - \frac{1}{L} \arctan \left(\frac{p + \rho \sin \frac{\theta}{2}}{-q + \rho \cos \frac{\theta}{2}} \right), \quad (22)$$

$$\kappa_I = \frac{1}{2L} \ln \eta = \frac{1}{2L} \ln \left(\left\{ -q + \rho \cos \frac{\theta}{2} \right\}^2 + \left\{ p + \rho \sin \frac{\theta}{2} \right\}^2 \right), \quad (23)$$

where $\rho = [(1 + q^2 - p^2)^2 + 4p^2 q^2]^{1/4}$. In order to compute the Bloch wave number, it is only necessary to evaluate Eqs. (22) and (23) for different values of the frequency. Fig. 3 compares how the variations on thickness in the metallic layers modify absorption and the band structure, and for verification is contrasted with the transmittance. We start with a metallic thickness of 5 nm, which some years ago was not considered as a realistic thickness according to the literature [5,32] whereas today for silver it is possible to grow ultrathin films at this size or below [33–35] even in the combination SiO₂/Si(100) [34,35] as substrate, but although controversial we include this image for the sake of comparison. Also, it is necessary to say that the band structure is an *ad infinitum* calculation, whereas the transmittance is only for 10 unit cells which is perfectly valid for these amounts of metal.

Fig. 3(a)–(c) shows a gradual change at the bottom of the first band. This is purely an effect of the absorption of the metal for low frequencies, i.e., before the plasma frequency all the frequencies will be attenuated or completely absorbed depending on the thickness of the metal; after that, waves with those frequencies can propagate without problems. This particular feature can be exploited as a filter for infrared light in optical applications [8]. Also, in the same figure the formation of a very narrow stop gap starts to appear between the dielectric stops gaps when the amounts of metal are increased. These new stop gaps are clearly visible around 2.0 and 4.0 in the frequency axis of the transmittance (see Fig. 3(a)). At the beginning, these band gaps are very thin and not completely defined in the transmittance but when the metal thickness is 10 nm, we can see them also there, as full stop gaps. Fig. 3(c) shows a full band gap centered near 2.0, another one around 4.0 and one more near 6.0, in the frequency

axis. This means that the metallic layers generate an additional band gap between the usual structural band gaps originated by the DPC substrate, in fact that is very remarkable because it is not predicted neither by medium theories [36] nor effective index of refraction approaches [37]. This very narrow band gap can be used, for example, as a very narrow filter for a particular bandwidth, just choosing one half of the central frequency of the signal as the Bragg frequency, thus the second harmonic of the Bragg frequency will be exactly the central frequency of the signal and therefore it will be located exactly in the middle of the metallic band gap. It is interesting to mention that very narrow stop gaps are also present in the Fibonacci stacks but the exact position of the stops gaps cannot be predicted and in general the transmittance profile is very complicated [25]. In contrast, a combination of a stack with a normal dielectric material and an exponential graded material in a Fibonacci sequence can generate very big stop gaps [27].

On the other hand, in Fig. 3(d), there is no longer a good coincidence between the band gaps and the transmittance. As transmittance is completely valid for these amounts of metal, band structures are no longer trusted and do not describe appropriately the behavior of the electromagnetic wave propagating in this medium. This is precisely the regime studied in Ref. [4]. The thickness of the metallic layers is big enough that cannot be considered a perturbation any longer.

4. Width and localization of band gaps

In this section, the procedure presented by Yeh [24] and explained in Section 2 is followed to calculate the maximum absorption for the 1D-MDPC and the width of the band gap. This will be done only for the band gaps that correspond to the metallic layers in the even harmonics of the Bragg frequency.

It is assumed that the metallic contribution to the phase will be small and condition $k_1 a = k_2 b = \pi/2$ is still valid with a slight modification. The dielectric band gaps are formed at odd ω_B , with a phase separation of 2π . Thus, as the metallic band gap is exactly at the middle of two dielectric ones, the condition should be modified to

$$k_1 a = k_2 b = \frac{\pi}{2} + \pi = \frac{3\pi}{2}, \quad (24)$$

This condition is valid whenever the thickness of the metal δ is small. Hence, the dispersion relation of the MDPC reduces to

$$\cos(\kappa L) = -\frac{1}{2} \frac{k_1^2 + k_2^2}{k_1 k_2} \cos(k_{3R} \delta). \quad (25)$$

In this case, Eq. (3) still holds, and therefore the dispersion relation changes to

$$\cos\left(\frac{\pi}{2} + i\kappa_I L\right) = -\frac{1}{2} \frac{k_1^2 + k_2^2}{k_1 k_2} [\cos(k_{3R} \delta) \cosh(k_{3I} \delta) - i \sin(k_{3R} \delta) \sinh(k_{3I} \delta)]. \quad (26)$$

Separating real and imaginary parts, the following equations are obtained:

$$\cosh(\kappa_I L) = \frac{1}{2} \frac{k_1^2 + k_2^2}{k_1 k_2} \cos(k_{3R} \delta) \cosh(k_{3I} \delta), \quad (27)$$

$$\sin(k_{3R} \delta) \sinh(k_{3I} \delta) = 0. \quad (28)$$

From these equations, the following restriction for k_{3R} follows:

$$k_{3R} \delta = 2n\pi, \quad (29)$$

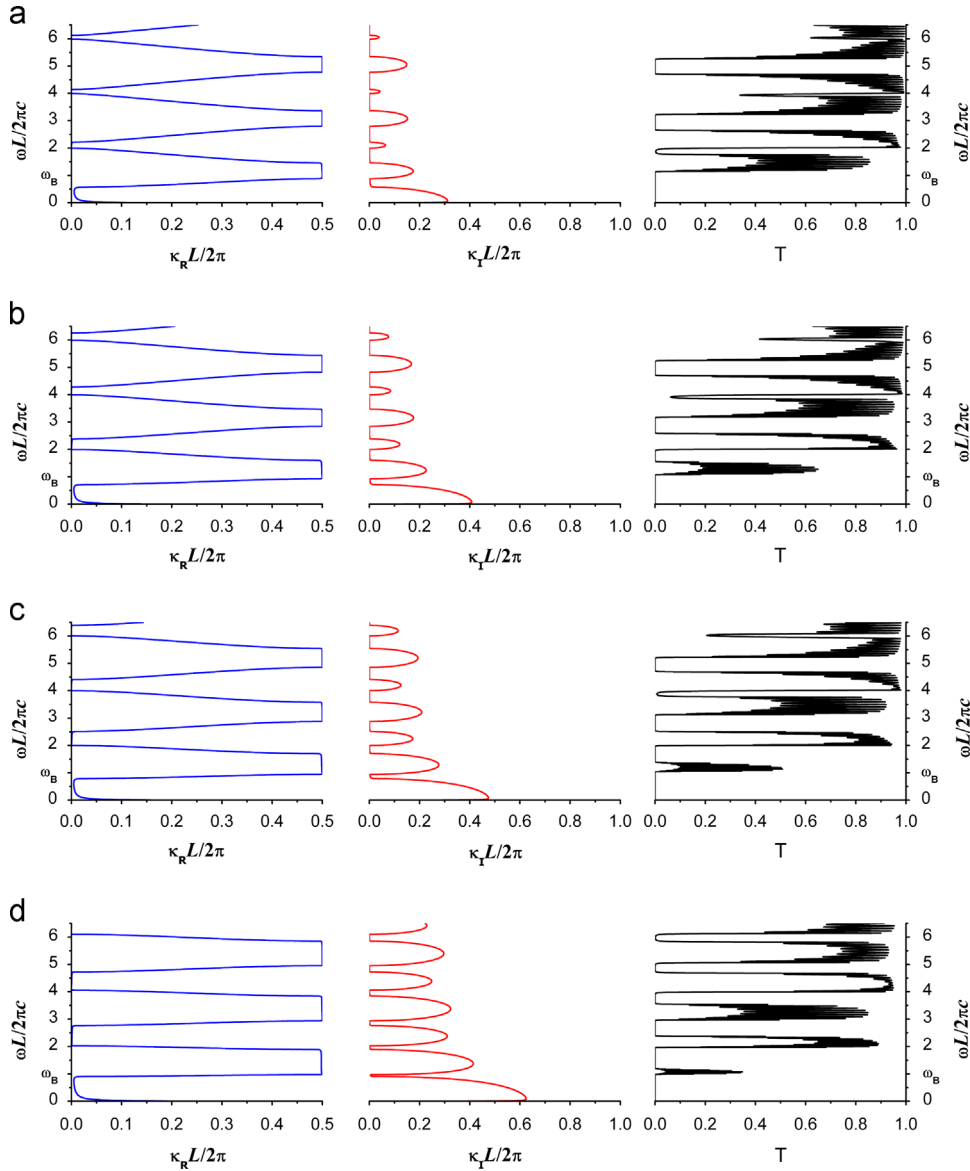


Fig. 3. Band structure, absorption and finally transmittance for different thicknesses of metal. From top to bottom: (a) $\delta=5$, (b) $\delta=10$, (c) $\delta=15$ and (d) $\delta=30$ nm.

with $n=0, 1, 2, 3, \dots$, given that Eq. (28) should be satisfied and κ_I should be positive (as defined by the equations) in Eq. (27). The maximum absorption from the metal in the middle of the band gap is given by

$$\kappa_I L = \operatorname{arccosh} \left(\frac{k_1^2 + k_2^2}{2k_1 k_2} [\cosh(k_{3I} \delta)] \right). \quad (30)$$

The expression is very similar to the one found for the dielectric case, Eq. (5), with a correction introduced for the metal and which depends directly on the thickness of the metallic sheet. In order to calculate the width of the metallic band gap, a small shift to the low frequencies is considered on the neighborhood of the Bragg frequency for the metallic stop gaps; then

$$k_1 a = k_2 b = \frac{3\pi}{2} + y, \quad (31)$$

$$k_{3R} \delta = 2n\pi + y. \quad (32)$$

Evaluating this expression in the dispersion relation (14), and taking into account that we are working in the boundaries of the first Brillouin zone ($\kappa_I=0$), the dispersion relation reduces to

$$\begin{aligned} & \left[\sin^2 y - \frac{k_1^2 + k_2^2}{k_1 k_2} \cos^2 y \right] [\cos y \cosh(k_{3I} \delta) - i \sin y \sinh(k_{3I} \delta)] \\ & - \frac{1}{k_3} \left[\frac{k_1^2 + k_3^2}{k_1} (-\cos y) \sin y + \frac{k_2^2 + k_3^2}{k_2} \sin y (-\cos y) \right] \\ & [\sin y \cosh(k_{3I} \delta) - i \cos y \sinh(k_{3I} \delta)] = -1. \end{aligned} \quad (33)$$

After some cumbersome algebra, the real and imaginary parts can be obtained

$$\begin{aligned} & \left[1 - \frac{(k_1 + k_2)^2}{2k_1 k_2} \cos^2 y \right] \cos y \cosh(k_{3I} \delta) + \frac{k_{3R}}{2|k_3|^2} \left[\frac{k_1^2 + |k_3|^2}{k_1} + \frac{k_2^2 + |k_3|^2}{k_2} \right] \\ & \sin^2 y \cos y \cosh(k_{3I} \delta) + \frac{k_{3I}}{2|k_3|^2} \left[\frac{k_1^2 - |k_3|^2}{k_1} + \frac{k_2^2 - |k_3|^2}{k_2} \right] \end{aligned}$$

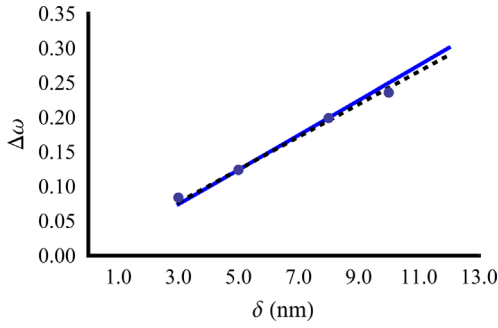


Fig. 4. Solid line, the width of the metallic band gap described by Eq. (38). Circles are numerical measurements and dashed line is a numerical fit.

$$\sin y \cos^2 y \sinh(k_{3I}\delta) = -1 \quad (34)$$

$$\left[\frac{(k_1 + k_2)^2}{2k_1 k_2} \cos^2 y - 1 \right] \sin y \sinh(k_{3I}\delta) + \frac{k_{3R}}{2|k_3|^2} \left[\frac{k_1^2 + |k_3|^2}{k_1} + \frac{k_2^2 + |k_3|^2}{k_2} \right] \sin y \cos^2 y \sinh(k_{3I}\delta) + \frac{k_{3I}}{2|k_3|^2} \left[\frac{|k_3|^2 - k_1^2}{k_1} + \frac{|k_3|^2 - k_2^2}{k_2} \right] \sin^2 y \cos y \cosh(k_{3I}\delta) = 0 \quad (35)$$

Up to this point, all the equations are exact. In order to obtain a simpler expression for the band gap width, it is necessary to introduce some approximations. Taking the expansions of the sine and cosine functions to zero-th order in Eq. (35)

$$\left[\frac{(k_1 + k_2)^2}{2k_1 k_2} - 1 \right] \sinh(k_{3I}\delta) + \frac{k_{3R}}{2|k_3|^2} \left[\frac{k_1^2 + |k_3|^2}{k_1} + \frac{k_2^2 + |k_3|^2}{k_2} \right] \sinh(k_{3I}\delta) + \frac{k_{3I}}{2|k_3|^2} \left[\frac{|k_3|^2 - k_1^2}{k_1} + \frac{|k_3|^2 - k_2^2}{k_2} \right] y \cosh(k_{3I}\delta) = 0 \quad (36)$$

which can be immediately solved to

$$y = \frac{(n_1^2 + n_2^2)|n_3|^2 + n_{3R}(n_1 n_2 + |n_3|^2)(n_1 + n_2)}{(n_1 + n_2)(n_1 n_2 - |n_3|^2)n_{3I}} \tanh(k_{3I}\delta) \quad (37)$$

and the width of the band gap is

$$\Delta\omega_{Mgap} = \frac{4\omega_B}{3\pi} y. \quad (38)$$

This last relation is plotted in Fig. 4 and compared with direct numerical measurements of the metallic band gap and also with the numerical fit, as can be seen the agreement is excellent. We are showing a range of nonrealistic bulk thickness [5,32–35], only for the sake of comparison. It is worth to mention that a recent work in two dimensional dielectric photonic crystals (2D-DPCs) and photonic quasicrystals (PQCs) a linear model is proposed to correlate the transverse magnetic band gap with three geometrical factors. Thus these geometrical factors, that play a major role in the width of the band gap for a fixed dielectric contrast, are the deviations of the noncircular shape in rot-like 2D-DPCs, the nonuniform particle distribution and the nonuniform neighbor particle distance ditribution [38,39]. These authors also studied how the filling factor, the rotational symmetry and experimental fabrication parameters affect the band gap in PQCs; they proposed a way to fabricate this cuasicrystals and showed some examples of the manufactured structures, with a good agreement between the theory and the experiment [40].

5. Conclusions

Summarizing, we demonstrated the existence of structural metallic band gaps in a ternary material, dielectric–dielectric–metal, and we derived analytical equations for their computation. Also, we showed the existence of metallic band gaps not only in the lowest band but also at high frequencies. These gaps are structural ones but different and additional to the dielectric ones in the DPC substrate as it was mentioned before. Furthermore, the enhancement in the band gap width that is present in MPC is also present in the MDPC that was studied, showing in this way that dielectric features and metallic ones coexist in this structure. Our results for oblique incidence for transversal electric and transversal magnetic modes will be published elsewhere.

Acknowledgments

The authors would like to thank Dr. Daniel A. May-Arrioja for his enlightening comments about a possible way of making the structure under study. D. L. Romero-Antequera would like to thank National Council for Science and Technology (CONACyT), Mexico, for the scholarship with number 211965/223982. This research was supported by CONACyT under Contract CB-2008/101378 “Acoplamiento De Plasmones Y Ondas Nolineales (Solitones Espaciales y Ondas Superficiales)”.

References

- [1] H.A. Macleod, Thin film optical filters, Series in Optics and Optoelectronics Series, Third Ed., Taylor & Francis, UK, ISBN 9780750306881, 2001 (<http://books.google.com.mx/books?id=DOS9hxpJq8C>).
- [2] J.D. Joannopoulos, S.G. Johnson, J.N. Winn, R.D. Meade, Photonic Crystals: Molding the Flow of Light, Second Ed., Princeton University Press, Singapore ISBN 9780691124568, 2008 (<http://books.google.com.mx/books?id=owhE36qiTP8C>).
- [3] V. Kuzmiak, A.A. Maradudin, Physical Review B 55 (12) (1997) 7427, <http://dx.doi.org/10.1103/PhysRevB.55.7427>.
- [4] H. Contopanagos, E. Yablonovitch, N.G. Alexopoulos, Journal of the Optical Society of America A 16 (9) (1999) 2294, <http://dx.doi.org/10.1364/JOSAA.16.002294> (<http://josaa.osa.org/abstract.cfm?URI=josaa-16-9-2294>).
- [5] M. Scalora, M.J. Bloemer, A.S. Pethel, J.P. Dowling, C.M. Bowden, A.S. Manka, Journal of Applied Physics 83 (5) (1998) 2377, <http://dx.doi.org/10.1063/1.366996>.
- [6] D. Soto-Puebla, M. Xiao, F. Ramos-Mendieta, Physics Letters A 326 (3–4) (2004) 273, <http://dx.doi.org/10.1016/j.physleta.2004.03.070> <http://dx.doi.org/10.1016/j.physleta.2004.03.070>.
- [7] M. Bergmair, M. Huber, K. Hingerl, Applied Physics Letters 89 (8) (2006) 081907, <http://dx.doi.org/10.1063/1.2338546> <http://dx.doi.org/10.1063/1.2338546>.
- [8] M. Bergmair, K. Hingerl, Journal of Optics A: Pure and Applied Optics 9 (9) (2007) S339, <http://dx.doi.org/10.1088/1464-4258/9/9/S09>.
- [9] G. Adamo, K. MacDonald, Y. Fu, C.-M. Wang, D. Tsai, F. García de Abajo, N. Zheludev, Physical Review Letters 103 (11) (2009), <http://dx.doi.org/10.1103/PhysRevLett.103.113901>.
- [10] S. Cavalcanti, M. de Dios-Leyva, E. Reyes-Gómez, L. Oliveira, Physical Review B 74 (15) (2006), <http://dx.doi.org/10.1103/PhysRevB.74.153102>.
- [11] S. Cavalcanti, M. de Dios-Leyva, E. Reyes-Gómez, L. Oliveira, Physical Review E 75 (2) (2007), <http://dx.doi.org/10.1103/PhysRevE.75.026607>.
- [12] J. Escobedo-Alatorre, J. Sánchez-Mondragón, M. Torres-Cisneros, R. Selvas-Aguilar, M. Basurto-Pensado, Optical Materials 27 (7) (2005) 1260, <http://dx.doi.org/10.1016/j.optmat.2004.11.021>.
- [13] J. Escobedo-Alatorre, J. Sánchez-Mondragón, M. Tecpoyotl-Torres, G. Martínez-Nikonoff, E. Alvarado-Mendez, SPIE—International Society for Optical Engineering (2003), <http://dx.doi.org/10.1117/12.507332>.
- [14] P. Yeh, A. Yariv, E. Marom, Journal of the Optical Society of America 68 (9) (1978) 1196, <http://dx.doi.org/10.1364/JOSA.68.001196>.
- [15] Y. Xu, W. Liang, A. Yariv, J.G. Fleming, S.-Y. Lin, Optics Letters 28 (22) (2003) 2144, <http://dx.doi.org/10.1364/OL.28.002144>.
- [16] A. Zamudio-Lara, J. Escobedo-Alatorre, J. Sánchez-Mondragón, M. Tecpoyotl-Torres, Optical Materials 27 (7) (2005) 1255, <http://dx.doi.org/10.1016/j.optmat.2004.11.020>.
- [17] A. Zamudio-Lara, J.J. Sánchez-Mondragón, M. Torres-Cisneros, J.J. Escobedo-Alatorre, C. Velásquez Ordoñez, M.A. Basurto-Pensado, L.A. Aguilera-Cortes, Optical Materials 29 (1) (2006) 60, <http://dx.doi.org/10.1016/j.optmat.2006.03.026>.
- [18] P. Yeh, A. Yariv, Ch.-Sh. Hong, Journal of the Optical Society of America 67 (4) (1977) 423, <http://dx.doi.org/10.1364/JOSA.67.000423>.

- [19] S.K. Awasthi, S.P. Ojha, Progress in Electromagnetics Research M 4 (2008) 117, <http://dx.doi.org/10.2528/PIERM08061302><http://dx.doi.org/10.2528/PIERM08061302>.
- [20] Y.-H. Chang, Ch.-Ch. Liu, T.-J. Yang, Ch.-J. Wu, Journal of the Optical Society of America B 26 (5) (2009) 1141, <http://dx.doi.org/10.1364/JOSAB.26.001141>.
- [21] Ch.-Ch. Liu, Y.-H. Chang, T.-J. Yang, Ch.-J. Wu, Progress in Electromagnetics Research 96 (2009) 329, <http://dx.doi.org/10.2528/PIER09090704>.
- [22] C.-J. Wu, Y.-H. Chung, B.-J. Syu, Progress in Electromagnetics Research 102 (2010) 81.
- [23] Ch.-Sh. Yuan, H. Tang, Ch. He, X.-L. Chen, X. Ni, M.-H. Lu, Y.-F. Chen, N.-B. Ming, Physica B: Condensed Matter 406 (10) (2011) 1983, <http://dx.doi.org/10.1016/j.physb.2011.02.071>.
- [24] P. Yeh, Optical waves in layered media, Wiley Series in Pure and Applied Optics, Wiley, New Jersey, USA. ISBN 9780471731924, 2005 (<http://books.google.com.mx/books?id=-yZBAQAIAAJ>).
- [25] R. Riklund, M. Severin, Journal of Physics C: Solid State Physics 21 (17) (1988) 3217, <http://dx.doi.org/10.1088/0022-3719/21/17/012>.
- [26] X.-H. Deng, J.-T. Liu, J.-H. Huang, L. Zou, N.-H. Liu, Journal of Physics: Condensed Matter 22 (5) (2010) 055403, <http://dx.doi.org/10.1088/0953-8984/22/5/055403>.
- [27] B.K. Singh, K.B. Thapa, P.C. Pandey, Optics Communications 297 (2013) 65, <http://dx.doi.org/10.1016/j.optcom.2012.12.053>.
- [28] A. Alejo-Molina, J.J. Sánchez-Mondragón, D.A. May-Arrioja, D. Romero, J. Escobedo-Alatorre, A. Zamudio-Lara, Microelectronics Journal 40 (3) (2009) 459, <http://dx.doi.org/10.1016/j.mejo.2008.06.020>.
- [29] L. Jia, E.L. Thomas, Physical Review A 84 (3) (2011) 033810-1, <http://dx.doi.org/10.1103/PhysRevA.84.033810>.
- [30] K. Dridi, A. Benhsaien, J. Zhang, T. Hall, Proceedings of SPIE, 8412, 84121R-1, 2012 <http://dx.doi.org/10.1117/12.2001459>. (<http://proceedings.spiedigitallibrary.org/proceeding.aspx?articleid=1387319>).
- [31] A. Alejo-Molina, J.J. Sánchez-Mondragón, A. Zamudio-Lara, D.A. May-Arrioja, M. Torres-Cisneros, Omnidirectional reflector in a ternary metallo-dielectric stack, in: Proceedings of Latin America Optics and Photonics Conference (LAOP), Optical Society of America, Washington, DC, paper WE26, 2010, Available from: (<http://dx.doi.org/10.1364/LAOP.2010.WE26>) A. Alejo-Molina, One dimensional metallo dielectric photonic crystal (Ph.D. thesis), National Institute for Astrophysics Optics and Electronics, Tonantzintla, Pue, 2010
- [32] P.B. Johnson, R.W. Christy, Physical Review B 6 (12) (1972) 4370, <http://dx.doi.org/10.1103/PhysRevB.6.4370>.
- [33] M. Gnanavel, C.S. Sunandana, Optical absorption and photoluminescence in ultra thin silver and silver iodide films, PhotonicsGlobal@Singapore, IPGC 2008, IEEE, pp. 1–4. <http://dx.doi.org/10.1109/IPGC.2008.4781352>. Available from: (http://ieeexplore.ieee.org/xpl/login.jsp?tp=&arnumber=4781352&url=http%3A%2F%2Fieeexplore.ieee.org%2Fxp%2Fabs_all.jsp%3Farnumber%3D4781352).
- [34] V.J. Logeeswaran, N.P. Kobayashi, M.S. Islam, W. Wu, P. Chaturvedi, N.X. Fang, S.Y. Wang, R.S. Williams, Nano Letters 9 (1) (2009) 178, <http://dx.doi.org/10.1021/nl8027476>.
- [35] N. Formica, D.S. Ghosh, A. Carrilero, T.L. Chen, R.E. Simpson, V. Pruneri, Applied Materials and Interfaces 5 (8) (2013) 3048, <http://dx.doi.org/10.1021/am303147w>.
- [36] A. Krokhin, P. Halevi, Physical Review B 53 (3) (1996) 1205, <http://dx.doi.org/10.1103/PhysRevB.53.1205>.
- [37] X. Xu, Y. Xi, D. Han, X. Liu, J. Zi, Z. Zhu, Applied Physics Letters 86 (9) (2005) 091112, <http://dx.doi.org/10.1063/1.1879101>.
- [38] L. Jia, I. Bitá, E.L. Thomas, Physical Review Letters 107 (19) (2011) 193901-1, <http://dx.doi.org/10.1103/PhysRevLett.107.193901>.
- [39] L. Jia, I. Bitá, E.L. Thomas, Physical Review A 84 (2) (2011) 023831-1, <http://dx.doi.org/10.1103/PhysRevA.84.023831>.
- [40] L. Jia, I. Bitá, E.L. Thomas, Advanced Functional Materials 22 (6) (2012) 1150, <http://dx.doi.org/10.1002/adfm.201101804>.